Original article

Curcumin can prevent the loss of sinoatrial node cells in methionine-treated rats: A stereological study

Atefeh Rahimi [a,b], Ali Rafati [a,b], Ali Noorafshan [a,c], Narges Karbalaei [a,b], Saied Karbalay-Doust [a,c,*]

[a] *Histomorphometry and Stereology Research Center, Shiraz University of Medical Sciences, Shiraz, Iran*
[b] *Department of Physiology, Shiraz University of Medical Sciences, Shiraz, Iran*
[c] *Department of Anatomy, Shiraz University of Medical Sciences, Shiraz, Iran*

A B S T R A C T

Methionine (MET) rich diets, smoking, coffee and alcohol consumption, low physical activity, and aging are related to high plasma concentrations of homocysteine, which can jeopardize the heart health. Although hyperhomocysteinemia has been considered a recognized risk factor for cardiac dysrhythmia, the structural changes of the conductive system, including Sinoatrial (SA) node of the heart involved in the disorder, have not been completely clarified. Curcumin is the main component of turmeric and has shown some cardioprotective effects.

This study aimed to evaluate the effect of curcumin on the structural changes of the SA node in L-MET-treated rats. These alterations were evaluated by means of stereological techniques, namely cavalieri principle for volume estimation and optical disector counting technique for cell counting. Both techniques used two-dimensional images for obtaining three-dimensional parameters. The rats were divided into four groups, including control, MET-treated (1 g/kg/day), curcumin-treated, (100 mg/kg/day), and MET + curcumin. The treatments were performed for 28 days. On the final day, SA nodes were dissected out for stereological investigation. Compared to the control rats, the volume of SA node, total volume of grape-like cell clusters, and number of SA node cells were respectively decreased by 42%, 34%, and 37% in the MET-treated group (p < 0.04). However, collagen density remained constant in all the study groups. Furthermore, treatment with curcumin could protect the SA node from cellular decline in the MET + curcumin group (p < 0.01).

It can be concluded that curcumin could prevent the structural changes of the SA node in the rats treated with methionine.

1. Introduction

Increment in plasma homocysteine level has been proposed to be a recently recognized risk factor for heart problems (Bokhari et al., 2005; Derouiche et al., 2014). High homocysteine levels can be seen in Methionine (MET) rich diets, such as the typical protein-rich western diet with a high content of meat, milk, and eggs. Other factors related to high plasma concentrations of homocysteine include smoking, coffee and alcohol consumption, low physical activity, and aging (Bokhari et al., 2005; Derouiche et al., 2014). Hyperhomocysteinemia may also originate from numerous genetic and environmental causes, such as gene mutation, vitamins B6, B12, and folate deficiency, renal failure, and medications (Bokhari et al., 2005; Derouiche et al., 2014). Hyperhomocysteinemia may stimulate structural problems of the heart including the conductive system through various potential mechanisms, including increment of the chance of coronary arteriosclerosis and myocardial infarction/ischemia, high troponin levels, oxidative stress, myocardial fibrosis, and conductive system dysfunction (Joseph et al., 2003; Walker et al., 2004). It has also been reported that hyperhomocysteinemia cases were at risk of arrhythmias (Ganguly and Alam, 2015; Kolling et al., 2011). Although hyperhomocysteinemia has been considered a culprit for cardiac dysrhythmia, the structural changes of the conductive

system, including the Sinoatrial (SA) node of the heart involved in the disorder, have not been completely clarified.

Nowadays, more attention is being paid to natural protective materials. Curcumin (CUR) is an herbal component and the main constituent of turmeric, which has anti-inflammatory (Shakeri and Boskabady, 2017), antihypercholesterolemic (Manjunatha and Srinivasan, 2007), and antioxidant properties, has been reported for its capability to scavenge reactive oxygen radicals (Ak and Gülçin, 2008), and has been considered an effective agent in the safety of cardiac cells during heart problems (Liu et al., 2017; Swamy et al., 2012).

Reactive Oxygen Species (ROS) are constantly generated during natural biological processes and eliminated by the antioxidant protective mechanism. Hyperhomocysteinemia causes an imbalance between the antioxidant defense and ROS. In this way, excessive ROS production leads to lipid peroxidation and oxidative stress, eventually damaging the cells. CUR can stop the generation of free radicals, act as a free radical scavenger and antioxidant, and prevent lipid peroxidation (Jagetia and Rajanikant, 2015; Kapoor et al., 2008). Since this compound is easily available, it was decided to evaluate its protective properties in the present study. SA node is the dominant pacemaker in the heart. SA node cells are located within a lattice of the connective tissue. The connective tissue insulates the SA node from the neighboring atrial cells. SA node cells are tiny in size and lighter than the nearby atrial cells. In addition, they have fewer mitochondria and myofibers as well as a smaller sarcoplasmic reticulum (Gómez-Torres et al., 2020; Nabipour, 2012).

The present research aimed to evaluate the main cells of the SA node after consumption of MET, inducing an approved rat model of hyperhomocysteinemia. It also aimed at evaluating the protective effects of CUR on the tissue alteration induced by MET. These alterations were evaluated using stereology, which is a subdivision of morphometry that relates there-dimensional parameters to two-dimensional measurements acquired on the sections of a structure. The following quantitative parameters were investigated using stereological techniques: volume of the SA node, total volume of the node cells clusters, total number (population) of the node cells, and density of the SA node's connective tissue.

2. Materials and methods

2.1. Animal model

A total of 32 male Sprague-Dawley rats were purchased from Experimental Animal Research Center of the University under the agreement and approval of the University's Research Vice-chancellor for standard animal caring (grant No. 1396-01-02-14701). The animals were housed in an air-conditioned room (temperature: 22 ± 2 °C, relative humidity: 50%) under a 12/12 h light/dark cycle.

2.2. Experimental design

The animals were subjected to an acclimatization period of two weeks before the beginning of the experiments. The 32 rats (250–300 g) were randomly allocated to four groups (n = 8), including control (phosphate buffer-treated animals), MET-treated (L-methionine, Sigma-Aldrich, Germany, 1 gr/kg/day) (Akgullu et al., 2015), CUR-treated (curcumin, Merck, Germany, 100 mg/kg/day) (Akgullu et al., 2015), and MET + CUR. It has been approved that the hyperhomocysteinemia model can be induced by MET nutritional overload (Hrnčić et al., 2014). The rats received the treatments orally for a period of 28 days. At the end of the experiment, the animals were euthanized with an overdose

intraperitoneal injection of ketamine–xylazine (Giroux et al., 2015). Then, their hearts were immediately removed and washed with saline.

2.3. Stereological evaluation

The right atrium (SA node region) was dissected out and kept in formalin buffer solution for three days (Gómez-Torres et al., 2020; Nabipour, 2012). After that, serial tissue sectioning (4 and 25 μm thickness) and staining (with hematoxylin-osin and Masson's tri-chrome stains) were carried out. It should be noted that the main cells of the SA node are normally organized in a dense collagen framework and tend to appear in grape-like clusters. The main cell is tiny and round or ovoid and has a hollow appearing cytoplasm with a large central nucleus (Gómez-Torres et al., 2020; Nabipour, 2012).

To quantify the parameters, a video-microscopy system and the stereology software designed at the University were used. To estimate the volume of the SA node "V(node)", the Cavalieri method was applied on the randomly sampled 4 μm sections of the SA node with the equal distance of "d". The total sectional areas "$\sum A$" of the SA node were traced and calculated using the software. Finally, the following formula was applied (Mühlfeld et al., 2010; Brown, 2017):

$$V(SA\ node) = \sum A \times d$$

To estimate the volume density "Vv" of the node cells (grape-like clusters) and the connective tissue, the point counting method was applied. In doing so, a point grid was lied on the image of the tissue and the densities were obtained using the following formula:

$$Vv = P(structure)/P(reference)$$

Where P(structure) represented the number of points lying on the favored structure and P(reference) was the total number of test points.

In order to obtain the cells population (numerical density), the optical disector method was applied using a Nikon Eclipse E200 microscope (Nikon, Japan) equipped with a 40X oil immersion objective lens (Nikon, Japan, Nikon Plan Fluor 40X oil immersion microscope objective with 1.3NA.) with high numerical aperture and a microcator (Heidenhain MT12 243602-01; Heidnehain, Nd 280, ID 636280-01, Germany). Afterwards, the 25 μm tissue sections were covered with a transparent unbiased counting frame. The numerical density of the node cells nuclei "N_V (nuclei/node)" was obtained using the following formula:

$$N_V(nuclei/node) = [\Sigma Q^-/(\Sigma P.(a/f).h)].(t/BA)$$

Where "ΣQ^-" was the total number of the sampled nuclei, "ΣP" was the total number of points hitting the node, "a/f" was the area per counting frame, "h" was the height of the disector, "t" was the mean section thickness measured and averaged at various locations of the section, and BA was the setting of the microtome for cutting the block. The "guard zones" and "h" were calculated according to the z-axis distribution of the nuclei (Mühlfeld et al., 2010; Brown, 2017). Finally, the total number or population of the nuclei was determined by multiplying "N_V (nuclei/node)" by "V(node)".

3. Statistical analysis

All analyses were performed using Graph Pad Prism software. Kruskal–Wallis and Mann-Whitney U tests was used to compare the study groups. Differences were considered significant at $p < 0.05$.

4. Results

4.1. Quantitative evaluation

The quantitative findings have been shown in Fig. 1. Accordingly, the volume of the SA node, total volume of the grape-like cell clusters, and number of SA node cells were respectively reduced by 42%, 34%, and 37% in the MET-treated group compared to the control rats (p < 0.04). However, the collagen density remained constant in all study groups. Furthermore, CUR showed protective effects on the rats receiving MET + CUR in comparison to the MET-treated ones (p < 0.01).

4.2. Qualitative evaluation

The results of qualitative evaluation of the SA node have been depicted in Fig. 2. Accordingly, shrunk cell clusters were seen in MET-treated rats. However, SA node cell clusters were safe in MET + CUR animals.

5. Discussion

This study investigated the effect of CUR on SA node structure in a rat model of MET-induced hyperhomocysteinemia. The primary section of the study showed that the main cells of the SA node underwent noticeable alterations after MET treatment in rats. Some studies have explained the functional disorders of the cardiac conductive system after hyperhomocysteinemia. However, the articles related to structural pathology have received less attention. In addition, there is limited research on SA node structure and cell population after hyperhomocysteinemia. In this context, the main reports have been concerned with cardiomyocytes changes. By way of illustration, the findings of the studies by Joseph et al. (2003) and Walker et al. (2004) suggested the loss of myocardial cells after the induction of hyperhomocysteinemia (Joseph et al., 2003; Walker et al., 2004), but they did not refer to node cells. Furthermore, Nechyporuk et al. (2020) reported that hyperhomocysteinemia was accompanied by hyperformation of ROS and damage of external mitochondrial membrane, resulting in the beginning of apoptotic cell death (Nechyporuk et al., 2020). Moreover, numerous studies have reported the functional changes of the heart after hyperhomocysteinemia. As a case in this point, Soni et al. (2016) demonstrated that hyperhomocysteinemia could induce alterations in the SA node function, atrioventricular nodes, and arrhythmias (Soni et al., 2016). The arrhythmias detected in hyperhomocysteinemia could be explained by the nodal cell loss observed in the present study (Soni et al., 2016).

The current study findings revealed a constant collagen content after MET-treatment. SA node is a mixed multi-partition structure defined by clusters of specialized cardiomyocytes embedded within connective tissue strands. Intranodal fibrosis has been considered a significant factor in SA node function and structure. The amount of fibrosis within the SA node increases with aging and cardiomegaly. In the present research, the whole cluster of the cells got shrunk without any changes in the connective tissue content
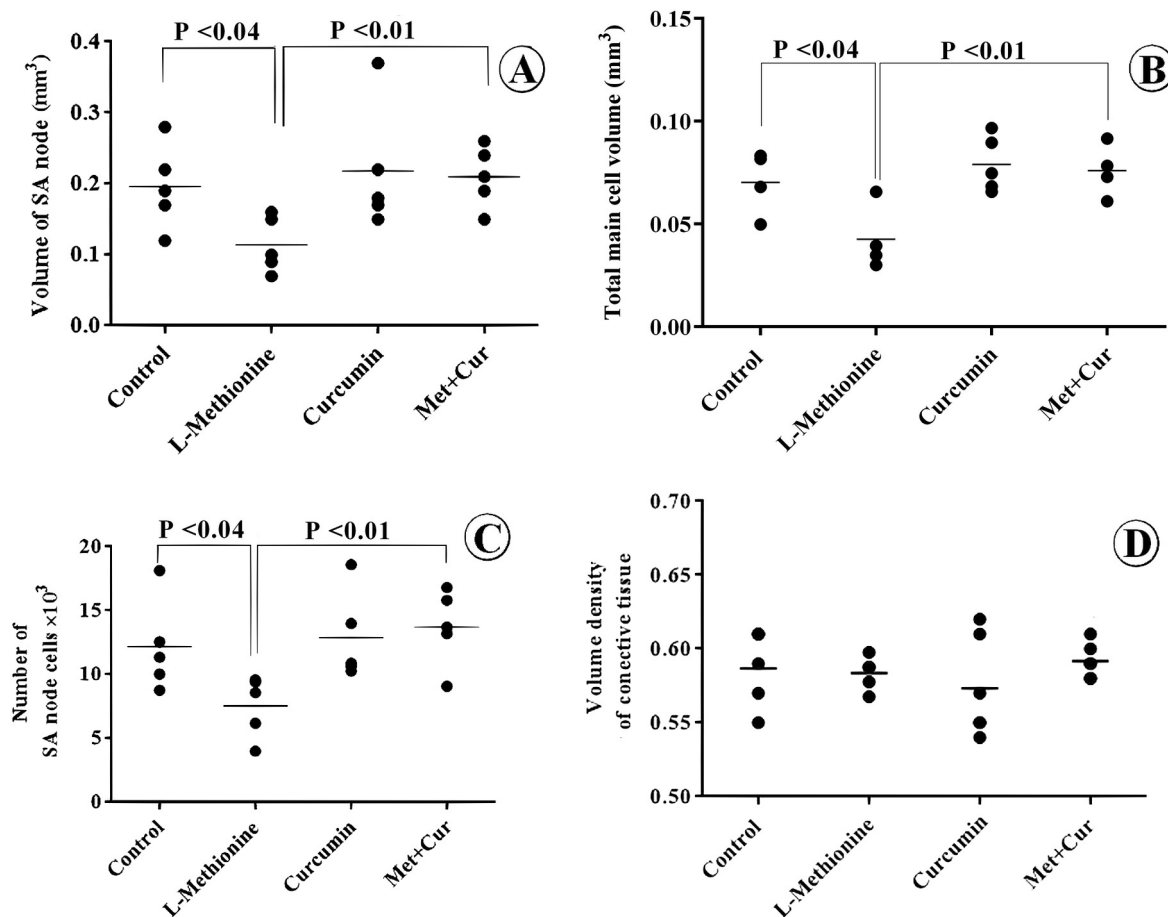

Fig. 1. Scatter plot of the structural parameters of the SA node in the experimental groups. The volume of the SA node **(A)**, the total volume of the grape-like clusters **(B)**, the population of the main cells **(C)**, and the volume density of the connective tissue lattice **(D)** in the control, methionine, curcumin, and methionine plus curcumin rats. Each dot represents an animal and the horizontal bars indicate the means of the parameters in the study groups. P-values have been mentioned on the plot.
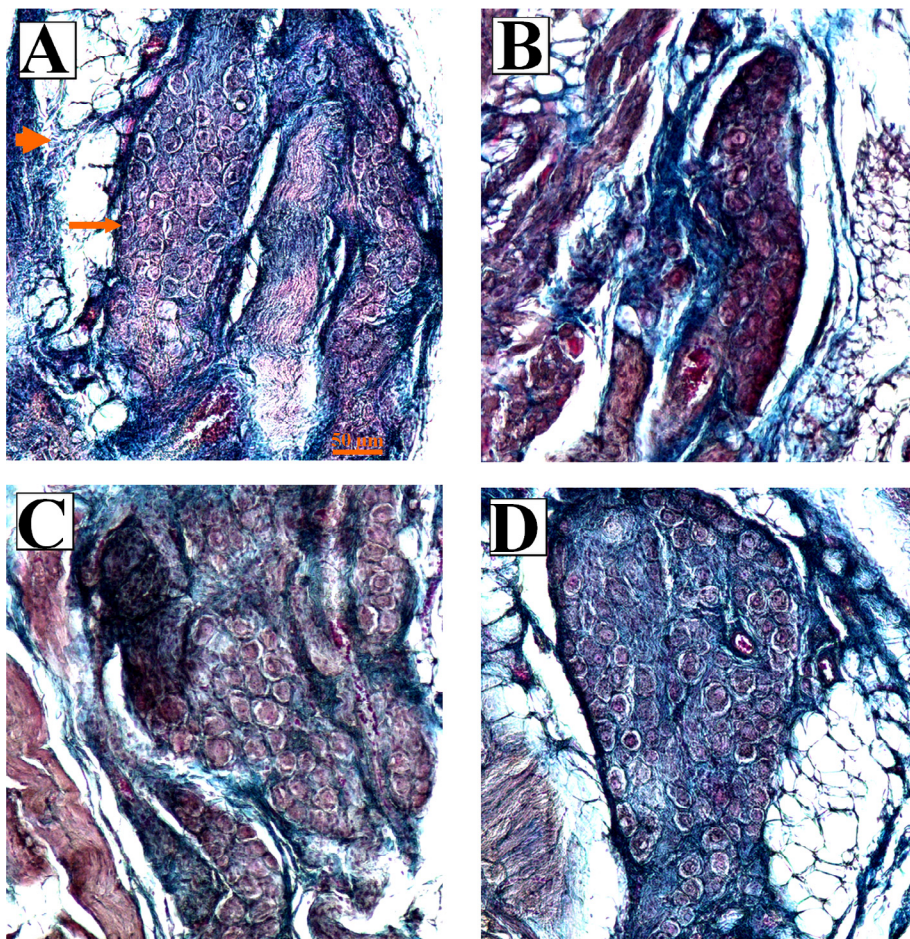
Fig. 2. Photomicrograph of the SA node in the experimental groups. (**A**) Control rats. The main cells of the SA node (long arrow) are normally organized in a dense collagen framework (short arrow). These cells tend to appear in grape-like clusters, with each cell being shaped much like a grape. The main cell is tiny and round or ovoid and has a hollow appearing cytoplasm with a large central nucleus. (**B**) In the methionine-treated rats, smaller grape-like clusters with smaller quantity of the main cells could be seen. (**C**) Curcumin-treated animals had similar parameters to those of the control group. (**D**) Treatment with methionine plus curcumin protected the grape-like clusters and their cells. Masson's trichrome stains. The scale bar is 50 μm.

(Csepe et al., 2015). Although there is little evidence in the literature about the mechanism of cell loss in the heart after hyperhomocysteinemia, the main pathological vascular findings have supposed the induction of oxidative damage to vascular endothelial cells and increased proliferation of vascular smooth muscle cells after oxidative stress (Kolling et al., 2011; Marcus et al., 2007; Brattstrom and Wilcken, 2000). Djuric et al. (2018) summarized that the aggravating properties of homocysteine were attained by several mechanisms, such as over-activation of *N*-methyl-d-aspartate receptors, Ca^{2+} management disorder, and amplified action of nicotinamide adenine dinucleotide phosphate-oxidase and the consequent surge of ROS creation (Djuric et al., 2018).

Oxidants are a main cause of cardiovascular injury and the consumption of antioxidants has been shown to prevent cardiac damage. As a result, CUR can be considered for the treatment of cardiovascular diseases due to its antioxidant properties. Many studies have investigated the protective effects of CUR on different types of cardiotoxicity (Sabet et al., 2020; Mohammed et al., 2020; Ahmed et al., 2020; Liu et al., 2019). Numerous studies have described the protective effects of CUR on cardiovascular diseases, including protection or mitigation against homocysteine–induced structural alterations. For instance, Li et al. (2016) indicated that CUR had protective effects on endothelial cells against homocysteine by preventing inflammation (Li et al., 2016). In the same line,

Ataie et al. (2010) reported that CUR could have a neuroprotective effect by reducing oxidative stress in the brain in a rat model of hyperhomocysteinemia (Ataie et al., 2010). Gorabi et al. (2019) also reported that CUR could have a cardio-protective effect by improving cardiac fibrosis (Gorabi et al., 2019). Based on the results of the present investigation, CUR improved the changes in the volume of the SA node, total volume of the grape-like cell clusters, and number of SA nodes in the MET-treated rats. The improvements in the listed parameters could be related to the antioxidant activity of CUR. These results were supported by the studies showing that CUR could protect the myocardial cells against free radical stress by inhibiting free radicals (Wei et al., 2019; He et al., 2018). MET-treatment could affect the SA node (grape-like clusters), and CUR could protect the structural changes.

Declaration of Competing Interest

The authors declare that they do not have any conflict of interest.

the MSc Degree in Physiology by Shiraz University of Medical Sciences and was financially supported by the Research Vice-chancellor of the University (grant No. 1396-01-02-14701). Hereby, the authors would like to thank Ms. A. Keivanshekouh at the Research Improvement Center of Shiraz University of Medical Sciences for improving the use of English in the manuscript.

References

Ahmed, O.A.A., El-Bassossy, H.M., Azhar, A.S., Tarkhan, M.M., El-Mas, M.M., 2020. Interference with AGEs formation and AGEs-induced vascular injury mediates curcumin vascular protection in metabolic syndrome. Sci. Rep. 10 (1). https://doi.org/10.1038/s41598-019-57268-z.

Ak, T., Gülçin, I., 2008. Antioxidant and radical scavenging properties of curcumin. Chem. Biol. Interact. 174 (1), 27–37. https://doi.org/10.1016/j.cbi.2008.05.003.

Akgullu, C., Huyut, M.A., Boyacioglu, M., Guleş, O., Eryilmaz, U., Hekim, T., Dogan, E., Zencir, C., Güngör, H., 2015. Nebivolol to attenuate the effects of hyper-homocysteinaemia in rats. Atherosclerosis. 240 (1), 33–39. https://doi.org/10.1016/j.atherosclerosis. 2015.02.054.

Ataie, A., Sabetkasaei, M., Haghparast, A., Hajizadeh Moghaddam, A., Ataie, R., Nasiraei Moghaddam, S.H., 2010. An investigation of the neuroprotective effects of Curcumin in a model of Homocysteine – induced oxidative stress in the rat's brain. Daru. 18 (2), 128–136.

Bokhari, S.W., Bokhari, Z.W., Zell, J.A., Lee, D.W., Faxon, D.P., 2005. Plasma homocysteine levels and the left ventricular systolic function in coronary artery disease patients. Coron. Artery. Dis. 16 (3), 153–161. https://doi.org/10.1097/00019501-200505000-00004.

Brattstrom, L., Wilcken, D.E., 2000. Homocysteine and cardiovascular disease: cause or effect?. Am. J. Clin. Nutr. 72 (2), 315–323. https://doi.org/10.1093/ajcn/72.2.315.Review.

Brown, D.L.m., 2017. Practical Stereology Applications for the Pathologist. Vet. Pathol. 54 (3), 358–368. https://doi.org/10.1177/0300985817695781. Review.

Csepe, T.A., Kalyanasundaram, A., Hansen, B.J., Zhao, J., Fedorov, V.V., 2015. Fibrosis: astructural modulator of sinoatrial node physiology and dysfunction. Front. Physiol. 6, 37. https://doi.org/10.3389/fphys.2015.00037. eCollection 2015.

Derouiche, F., Bôle-Feysot, C., Naïmi, D., Coëffier, M., 2014. Hyperhomocysteinemia-induced oxidative stress differentially alters proteasome composition and activities in heart and aorta. Biochem. Biophys. Res. Commun. 452 (3), 740–745. https://doi.org/10.1016/j.bbrc.2014.08.141.

Djuric, D., Jakovljevic, V., Zivkovic, V., Srejovic, I., 2018. Homocysteine and homocysteine-related compounds: an overview of the roles in the pathology of the cardiovascular and nervous systems. Can. J. Physiol. Pharmacol. 96 (10), 991–1003. https://doi.org/10.1139/cjpp-2018-0112.

Ganguly, P., Alam, S.F., 2015. Role of homocysteine in the development of cardiovascular disease. Nutr. J. 14, 6. https://doi.org/10.1186/1475-2891-14-6. Review.

Giroux, M.C., Hélie, P., Burns, P., Vachon, P., 2015. Anesthetic and pathological changes following high doses of ketamine and xylazine in Sprague Dawley rats. Exp. Anim. 64 (3), 253–260. https://doi.org/10.1538/expanim.14-0088.

Gómez-Torres, F.A., Sebastian, R., Ruíz-Sauri, A., 2020. Morphometry and comparative histology of sinus and atrioventricular nodes in humans and pigs and their relevance in the prevention of nodal arrhythmias. Res. Vet. Sci. 128, 275–285. https://doi.org/10.1016/j.rvsc.2019.12.008.

Gorabi, A.M., Hajighasemi, S., Kiaie, N., Rosano, G.M.C., Sathyapalan, T., Al-Rasadi, K., Sahebkar, A., 2019. Anti-fibrotic effects of curcumin and some of its analogues in the heart. Heart. Fail. Rev. 25 (5), 731–743. https://doi.org/10.1007/s10741-019-09854-6.

He, H., Luo, Y., Qiao, Y., Zhang, Z., Yin, D., Yao, J., You, J., He, M., 2018. Curcumin attenuates doxorubicin-induced cardiotoxicity via suppressing oxidative stress and preventing mitochondrial dysfunction mediated by 14–3-3gamma. Food. Funct. 9 (8), 4404–4418. https://doi.org/10.1039/c8fo00466h.

Hrnčíč, D., Rašić-Marković, A., Stojković, T., Velimirović, M., Puškaš, N., Obrenović, R., Macut, D., Sušić, V., Jakovljević, V., Djuric, D., Petronijević, N., Stanojlović, O., 2014. Hyperhomocysteinemia induced by methionine dietary nutritional overload modulates acetylcholinesterase activity in the rat brain. Mol. Cell. Biochem. 396 (1–2), 99–105. https://doi.org/10.1007/s11010-014-2146-8.

Jagetia, G.C., Rajanikant, G.K., 2015. Curcumin Stimulates the Antioxidant Mechanisms in Mouse Skin Exposed to Fractionated gamma-Irradiation. Antioxidants (Basel) 4 (1), 25–41. https://doi.org/10.3390/antiox4010025.

Joseph, J., Joseph, L., Shekhawat, N.S., Devi, S., Wang, J., Melchert, R.B., Hauer-Jensen, M., Kennedy, R.H., 2003. Hyperhomocysteinemia leads to pathological ventricular hypertrophy in normotensive rats. Am. J. Physiol. Heart. Circ. Physiol. 285 (2), H679–H686. https://doi.org/10.1152/ajpheart.00145.2003.

Kapoor, P., Ansari, M.N., Bhandari, U., 2008. Modulatory effect of curcumin on methionine-induced hyperlipidemia and hyperhomocysteinemia in albino rats. Indian. J. Exp. Biol. 46 (7), 534–540.

Kolling, J., Scherer, E.B., da Cunha, A.A., da Cunha, M.J., Wyse, A.T., 2011. Homocysteine induces oxidative-nitrative stress in heart of rats: prevention by folic acid. Cardiovasc. Toxicol. 11 (1), 67–73. https://doi.org/10.1007/s12012-010-9094-7.

Li, J., Luo, M., Xie, N., Wang, J., Chen, L., 2016. Curcumin protects endothelial cells against homocysteine induced injury through inhibiting inflammation. Am. J. Transl. Res. 8 (11), 4598–4604. eCollection 2016..

Liu, Q., Yuan, J.W., Zhang, F., Qiao, F., Sui, X.F., Liu, C.H., 2019. Curcumin protects rat H9C2 cardiomyocytes against doxorubicin toxicity by modulating oxidative stress and apoptosis. J. Biol. Regul. Homeost. Agents. 33 (6), 1849–1854. https://doi.org/10.23812/19-365-L.

Liu, H., Wang, C., Qiao, Z., Xu, Y., 2017. Protective effect of curcumin against myocardium injury in ischemia reperfusion rats. Pharm. Biol. 55 (1), 1144–1148. https://doi.org/10.1080/13880209.2016.1214741.

Manjunatha, H., Srinivasan, K., 2007. Hypolipidemic and antioxidant effects of dietary curcumin and capsaicin in induced hypercholesterolemic rats. Lipids. 42 (12), 1133–1142. https://doi.org/10.1007/s11745-007-3120-y.

Marcus, J., Sarnak, M.J., Menon, V., Verma, S., 2007. Homocysteine lowering and cardiovascular disease risk: lost in translation. Can. J. Cardiol. 23 (9), 707–710. https://doi.org/10.1016/S0828-282X(07)70814-0.

Mohammed, H.S., Hosny, E.N., Khadrawy, Y.A., Magdy, M., Attia, Y.S., Sayed, O.A., AbdElaal, M., 2020. Protective effect of curcumin nanoparticles against cardiotoxicity induced by doxorubicin in rat. Biochim. Biophys. Acta Mol. Basis. Dis. 1866 (5). https://doi.org/10.1016/j.bbadis.2020.165665.

Mühlfeld, C., Nyengaard, J.R., Mayhew, T.M., 2010. A review of state-of-the-art stereology for better quantitative 3D morphology in cardiac research. Cardiovasc. Pathol. 19 (2), 65–82. https://doi.org/10.1016/j.carpath.2008.10.015.

Nabipour, A., 2012. Comparative histological structure of the sinus node in mammals. Turk. J. Vet. Anim. Sci. 36 (5), 463–469 https://doi:10.3906/vet-0807-2.

Nechyporuk, V., Korda, M., Pentiuk, L., Kovalchuk, O., Andriichuk, V., 2020. Implementation of programmed cell death in circulating neutrophils and its special characteristics in experimentally induced hyperhomocysteinemia in a setting of thyroid dysfunction. Pol. Merkur. Lekarski. 48 (288), 437–442.

Sabet, Nima Shokouhi, Atashbar, Saman, Khanlou, Elham Mohammad, Kahrizi, Farzad, Salimi, Ahmad, 2020. Naunyn Schmiedebergs Arch Pharmacol. Curcumin attenuates bevacizumab-induced toxicity via suppressing oxidative stress and preventing mitochondrial dysfunction in heart mitochondria. Arch. Pharmacol. 393 (8), 1447–1457. https://doi.org/10.1007/s00210-020-01853-x.

Shakeri, Farzaneh, Boskabady, Mohammad Hossein, 2017. Anti-inflammatory, antioxidant, and immunomodulatory effects of curcumin in ovalbumin-sensitized rat. Biofactors. 43 (4), 567–576. https://doi.org/10.1002/biof.v43.410.1002/biof.1364.

Soni, C.V., Tyagi, S.C., Todnem, N.D., Givvimani, S., Pushpakumar, S.B., Villafane, J., Maldonado, C., 2016. Hyperhomocysteinemia alters sinoatrial and atrioventricular nodal function: Role of magnesium in attenuating these effects. Cell. Biochem. Biophys. 74 (1), 59–65. https://doi.org/10.1007/s12013-015-0711-8.

Swamy, A.V., Gulliaya, S., Thippeswamy, A., Koti, B.C., Manjula, D.V., 2012. Cardioprotective effect of curcumin against doxorubicin-induced myocardial toxicity in albino rats. Indian. J. Pharmacol. 44 (1), 73–77. https://doi.org/10.4103/0253-7613.91871.

Walker, E., Black, J., Parris, C., Bryda, E.C., Cansino, S., Hunt, L., Chappell, J., Wehner, P., Studeny, M., Wright, G.L., 2004. Effect of experimental hyperhomocysteinemia on cardiac structure and function in the rat. Ann. Clin. Lab. Sci. 34 (2), 175–180.

Wei, W., Peng, J., Li, J., 2019. Curcumin attenuates hypoxia/reoxygenation-induced myocardial injury. Mol. Med. Rep. 20 (6), 4821–4830. https://doi.org/10.3892/mmr.2019.10742.